Selective irradiation of the vascular endothelium has no effect on the survival of murine intestinal crypt stem cells

Bradley W. Schuller*, Peter J. Binns†, Kent J. Riley†, Ling Ma‡, M. Frederick Hawthorne‡§, and Jeffrey A. Coderre*¶

*Department of Nuclear Science and Engineering, and †Nuclear Reactor Laboratory, Massachusetts Institute of Technology, Cambridge, MA 02139; and ‡Department of Chemistry and Biochemistry, University of California, Los Angeles, CA 90024

Contributed by M. Frederick Hawthorne, January 9, 2006

The possible role of vascular endothelial cell damage in the loss of intestinal crypt stem cells and the subsequent development of the gastrointestinal (GI) syndrome is addressed. Mice received whole-body epithermal neutron irradiation at a dose rate of 0.57 ± 0.04 Gy·min^{-1}. An additional dose was selectively targeted to endothelial cells from the short-ranged (5–9 μm) particles released from neutron capture reactions in ^{10}B confined to the blood by incorporation into liposomes 70–90 nm in diameter. Different liposome formulations produced 45 ± 7 or 118 ± 12 μg/g ^{10}B in the blood at the time of neutron irradiation, which resulted in total absorbed dose rates in the endothelial cells of 1.08 ± 0.09 or 1.90 ± 0.16 Gy·min^{-1}, respectively. At 3.5 d after irradiation, the intestinal crypt microcolony assay showed that the 2- to 3-fold increased doses to the microvasculature, relative to the nonspecific whole-body neutron beam doses, caused no additional crypt stem cell loss beyond that produced by the neutron beam alone. The threshold dose for death from the GI syndrome after neutron-beam-only irradiation was 9.0 ± 0.6 Gy. There were no deaths from the GI syndrome, despite calculated absorbed doses to endothelial cells as high as 27.7 Gy, in the groups that received neutron beam doses of <9.0 Gy with boronated liposomes in the blood. These data indicate that endothelial cell damage is not causative in the loss of intestinal crypt stem cells and the eventual development of the GI syndrome.

gastrointestinal syndrome | boron | liposomes | neutron capture

Radiation-induced changes seen in normal tissues are traditionally separated into early and late effects. Stem-cell-based, rapidly renewing normal tissues, such as the bone marrow and the intestinal epithelium, are early responding tissues in which the time courses of the radiation syndromes are directly related to the turnover time of the differentiated functional cell compartments. The intestinal stem cells reside in the crypts of Lieberkühn at the base of the finger-like villi that comprise the intestinal epithelium. Epithelial cells differentiate as they migrate up the crypt and the villus and are eventually sloughed off at the tip into the intestinal lumen: the transit time takes ≈3–4 d. In the mouse small intestine, a wave of apoptosis is observed in what are thought to be crypt stem cells (1) as early as 3–6 h after irradiation with doses as low as 0.01 Gy (2). This effect saturates at ≈1 Gy. Higher doses are postulated to deplete the first few generations of differentiated transit cells that still retain the ability to revert to fully functional stem cells (2). Individual crypts are not sterilized until all of the actual and potential stem cells are inactivated, which occurs at doses of ≈8 Gy or higher. The crypt microcolony assay measures the survival of the last individual potential stem cells within each crypt (3). This assay involves counting the number of regenerating crypt-like foci per intestinal circumference 3–4 d after irradiation. The survival of one or more clonogenic cells per crypt allows its regeneration. Doses above ≈15 Gy sterilize virtually all of the crypt stem cells, resulting in complete loss of the intestinal villi and death from the gastrointestinal (GI) syndrome in ≈4–5 d. It has traditionally been assumed that the GI syndrome results from the direct killing of the rapidly growing stem cells, depletion of the differentiated parenchymal cells, and subsequent loss of tissue function (2, 4).

The GI syndrome has, however, recently been suggested to be a direct consequence of an early (4 h) wave of apoptosis in the intestinal vascular endothelial cells (5). These authors irradiated mice with single, whole-body photon doses of 15 Gy, which is sufficient to cause death from the GI syndrome, and demonstrated that it was possible to change the mode of death from the GI syndrome to the bone marrow syndrome (in effect, producing ≈3 Gy of radioprotection) when endothelial cell apoptosis was suppressed genetically by deletion of the gene for acid sphingomyelinase, which controls endothelial cell apoptosis through a ceramide pathway, or pharmacologically by administration of basic fibroblast growth factor. The precise mechanism of this proposed linkage between intestinal endothelial cell apoptosis and crypt stem cell depletion leading to the GI syndrome remains unproven (6–8).

An approach for the selective irradiation of the vascular endothelium that allows mechanistic studies into the role of endothelial cell damage in normal tissue radiation responses (9–12) has been applied in this report to crypt stem cell loss in the mouse small intestine. The method is based on the short-ranged (5–9 μm) alpha and lithium particles released from the neutron capture reaction in the stable minor isotope of boron: ^{10}B. When ^{10}B was restricted to the blood by incorporation into liposomes that could not diffuse into the surrounding tissues, absorbed dose in the microvasculature was increased relative to the uniform dose delivered by the neutron beam to the rest of the body. It is reported here that for both intestinal crypt stem cell survival and mode of death, there were no differences between the groups that were irradiated with the neutron beam alone and those that received the same beam dose and a substantially higher dose selectively delivered to the microvasculature.

Results

Biodistribution. The variation in the blood–boron concentration between 15 and 60 min after injection of the K^+ [*nido*-7-$CH_3(CH_2)_{15}$-7,8-$C_2B_9H_{11}]^{1-}$ (MAC) liposome preparation is shown in Fig. 1. At 30 min after injection, the boron concentration in blood was found to be 45 ± 7 μg/g ^{10}B. The ^{10}B

Conflict of interest statement: No conflicts declared.

Freely available online through the PNAS open access option.

Abbreviations: BPA, *p*-boronophenylalanine; BSH, $Na_2B_{12}H_{11}SH$; GI, gastrointestinal; LET, linear energy transfer; MAC, K^+ [*nido*-7-$CH_3(CH_2)_{15}$-7,8-$C_2B_9H_{11}]^{1-}$; TAC, $[B_{20}H_{17}NH_3]^{3-}$.

§To whom correspondence may be addressed. E-mail: mfh@chem.ucla.edu.

¶To whom correspondence may be addressed at: Department of Nuclear Science and Engineering, Massachusetts Institute of Technology, 150 Albany Street, NW14-2211, Cambridge, MA 02139. E-mail: coderre@mit.edu.

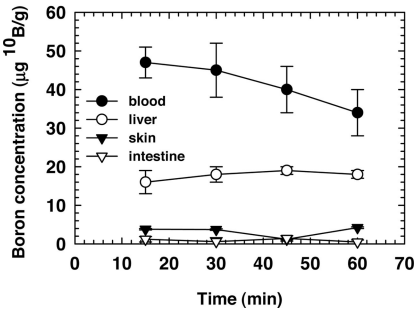

Fig. 1. ^{10}B concentrations in blood and tissues as a function of time after injection of 0.2 ml of the MAC liposome preparation into the retroorbital sinus. Points represent the mean ± SD (n = 5 mice per time point).

Table 1. Beam doses, total blood doses, and endothelial cell doses used in the survival experiments

Beam-only dose, Gy	^{10}B in blood,* μg/g ^{10}B	Total blood dose,† Gy	Endothelial cell dose,‡ Gy
5.7 ± 0.4	45 ± 7	20.9 ± 1.0	10.8 ± 0.9
7.5 ± 0.5	118 ± 12	60.1 ± 5.7	25.0 ± 2.0
8.3 ± 0.6	118 ± 12	66.5 ± 6.3	27.7 ± 2.2
9.0 ± 0.6	0	9.0 ± 0.6	9.0 ± 0.6
10.0 ± 0.7	0	10.0 ± 0.7	10.0 ± 0.7

*MAC liposomes or MAC+TAC liposomes were used to produce 45 ± 7 or 118 ± 12 μg/g ^{10}B in the blood, respectively.
†Total blood dose is the beam dose plus the ^{10}B dose to the blood.
‡Endothelial cell dose is the beam dose plus one-third of the ^{10}B dose to the blood.

concentrations in liver, skin, and small intestine were 18 ± 2, 3.7 ± 0.2, and 0.6 ± 1.0 μg/g ^{10}B, respectively. The low boron concentrations observed in the skin and intestine are most likely due to the blood content of the tissue samples analyzed. The time of irradiation was chosen as 30 min after injection based on the boron biodistribution and the logistical reasons associated with the reactor irradiations. The solution containing liposomes with MAC in the lipid bilayer and $[B_{20}H_{17}NH_3]^{3-}$ (TAC) in the interior (MAC+TAC) was used to provide a higher blood–boron concentration. Eight additional mice received a 0.2-ml injection of the MAC+TAC liposome preparation and were killed at 30 min after injection. The ^{10}B concentrations in blood, liver, and small intestine were 118 ± 12, 61 ± 3, and 0.54 ± 0.49 μg/g ^{10}B, respectively. As expected, the blood–boron concentration scaled proportionately with the increased boron content in the MAC+TAC liposome solution. The boron concentration in the small intestine was below the prompt gamma neutron activation analysis detection limit, as was the case for the MAC liposomes.

A time point 2 hr after injection was chosen for the p-boronophenylalanine (BPA) biodistribution study to allow the boron to equilibrate from the blood into the normal tissues. The ^{10}B concentrations in blood and small intestine were 13.7 ± 4.6 and 13.0 ± 3.6 μg/g ^{10}B, respectively (n = 5).

Dosimetry. The total absorbed dose rate in the epithermal neutron beam was 0.57 ± 0.04 Gy·min^{-1} at a depth of 2.5 cm and was composed of 77% low-linear energy transfer (LET) photons and 23% high-LET radiations, which are principally protons arising from thermal neutron capture in nitrogen. The relative uncertainty on the neutron beam doses was 2.2%, which includes only the statistical uncertainty in the beam monitor counts and variations of ≈1 mm in the positioning of the irradiation jig along the center of the beam's central axis. The additional absorbed dose rate from the ^{10}B capture reaction was 3.3 ± 0.18 cGy·min^{-1} per μg of ^{10}B present.

The total absorbed dose rate in the vascular endothelial cells, with boronated liposomes in the blood at the time of neutron irradiation, was estimated as the sum of the whole-body neutron beam absorbed dose rate plus one-third of the ^{10}B absorbed dose rate in the blood (Table 1). The additional absorbed dose rate in the microvasculature coming from boron neutron capture reactions in the blood was 1.1 ± 0.06 cGy·min^{-1} per μg of ^{10}B, which includes the geometrical factor of one-third (13). The higher ^{10}B concentration in the blood associated with the MAC+TAC liposomes allowed the dose to the vascular endothelial cells to be increased while all other parameters were held constant. Thus, the total absorbed dose rate in the microvasculature was 1.08 ± 0.09 or 1.90 ± 0.16 Gy·min^{-1} with 45 ± 7 or 118 ± 12 μg/g ^{10}B in the blood, respectively. The stated uncertainties on the microvascular absorbed dose rates include the uncertainty in the neutron beam dosimetry as well as the uncertainty in the blood–boron concentration at the time of irradiation.

Intestinal Crypt Regeneration Assay. The numbers of regenerating crypts per intestinal cross section as a function of the physical absorbed doses from the epithermal neutron beam are shown in Fig. 2 for the four experimental groups (epithermal neutron beam only, irradiation with the MAC liposomes in the blood, irradiation with the MAC+TAC liposomes in the blood, or the BPA positive control). The crypt regeneration data points for the two groups that received liposome injections and beam doses of >6 Gy were within one standard deviation of the exponential fit to the beam-only dose–response data (Fig. 2) despite the presence of 45 ± 7 or 118 ± 12 μg/g ^{10}B in the blood and estimated endothelial cell doses that were 2- or 3-fold higher than the whole-body beam doses (Table 1). Regression fits of the beam-only and the beam-plus-liposome data in the linear region of the dose–response relationship indicate that absorbed doses of 7.3 ± 0.6 Gy (beam only), 7.2 ± 0.6 Gy (beam plus MAC), and 7.1 ± 0.6 Gy (beam plus MAC+TAC) were required to reduce crypt stem cell survival to the level of 20 regenerating crypts per circumference. The added absorbed dose selectively delivered to the vascular endothelial cells in the beam-plus-liposome groups did not contribute to intestinal crypt stem cell depletion. Liposome injections with no neutron irradiation had no effect on crypt regeneration numbers compared with the nontreated controls.

The data shown in Fig. 2 are in good agreement with the data

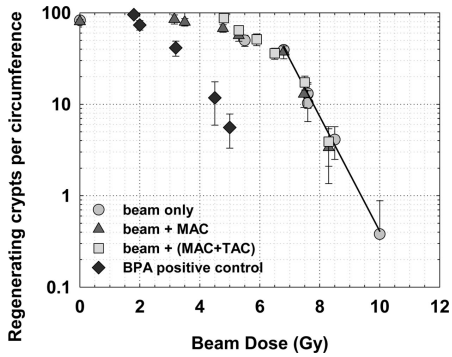

Fig. 2. Number of regenerating crypts per intestinal circumference as a function of neutron beam dose 84 ± 1 h after whole-body irradiation in the presence or absence of boronated liposomes in the blood or with a uniform ^{10}B distribution using BPA. The triangles and squares represent irradiation conditions where the dose to the microvasculature was increased relative to the rest of the mouse by a factor of 2 or 3, respectively. Points represent the mean ± SD of at least 16 jejunal cross sections, 4 sections from each of 4 mice.

of Gueulette *et al*. (14) in the same mouse (BALB/c) with the same irradiation jig and geometry in the same neutron beam. In that study (14), the epithermal neutron beam at the Massachusetts Institute of Technology Nuclear Reactor Laboratory was shown to have a relative biological effectiveness of 1.5 ± 0.04, relative to 6-MV photons, for the crypt regeneration endpoint. Thus, the neutron beam absorbed doses of 3.2–10.0 Gy used here, which are a mix of high- and low-LET radiations, correspond to photon-equivalent doses of 4.8–15.0 Gy for the crypt survival endpoint. Fig. 2 shows that there were <10 regenerating crypts per circumference for an absorbed dose of 8.3 Gy (a 12.5-Gy photon equivalent), which is consistent with this dose being near the threshold for a GI death.

The number of regenerating crypts per intestinal cross section after neutron irradiation in the presence of a uniform ^{10}B concentration in blood and intestine, as delivered by BPA, is also shown in Fig. 2. The intent of this BPA positive control experiment was to estimate the sensitivity of the crypt regeneration assay for the detection of potential ^{10}B diffusion out of the vessels. The presence of ≈13 μg/g ^{10}B in both blood and intestine increased the physical absorbed dose rate by 75%, an additional 0.43 Gy·min^{-1}. The BPA positive control dose–response curve is shifted significantly to the left when plotted versus the beam dose (Fig. 2). Based on these data, we estimate that the crypt regeneration assay could detect the effect of the added ^{10}B dose from as little as 2 μg/g ^{10}B outside the vessels, which represents a <2% "leakage" of the MAC+TAC blood–boron concentration.

Even with all ^{10}B restricted to the vessel lumen, the ranges of the alpha (9 μm) and lithium particles (5 μm) are such that some dose will be absorbed outside of the vessel wall. Monte Carlo simulations show that the ^{10}B dose gradient outside the vessel drops off steeply. For example, for the 8.3-Gy beam dose with the MAC+TAC liposomes (118 μg/g ^{10}B in the blood) (Table 1), the absorbed ^{10}B dose to the blood inside the vessel lumen is 58.2 Gy. Outside the vessel, at distances of 2, 5, and 7 μm from the vessel wall, the ^{10}B dose component is 3.0, 0.2, and 0.005 Gy, respectively. However, the crypt microcolony assay results (Fig. 2) indicate that this potential penetration of the particle dose outside the vessel had no detectable effect on the crypt stem cell survival.

Mouse Survival. Fig. 3*A* shows the survival of the beam-only groups as a function of time after whole-body neutron beam irradiation. All mice (n = 12) given 5.7 Gy and eight of 10 mice given 7.5 Gy lived beyond 30 d, indicating that these beam doses were below the LD_{50} for death from the bone marrow syndrome. At neutron beam doses of 8.3, 9.0, and 10.0 Gy, all mice (n = 28 total) died within 4–9 d (Fig. 3*A*). Fig. 4 shows hematoxylin-and-eosin-stained histological sections of small intestine (jejunum) and bone marrow from mice in the 8.3- and 9.0-Gy beam-only groups that were killed 9 and 5 d after irradiation, respectively. The intestinal mucosa was well on the way to recovery in the mouse that received the 8.3-Gy beam-only dose, whereas the intestinal epithelium was severely denuded in the mouse that received the 9.0-Gy beam-only dose, which is indicative of death from the GI syndrome. The bone marrow was severely depleted and showed extensive necrosis of the matrix and widespread hemorrhaging in both mice. Thus, the histopathology from the neutron beam-only irradiation groups indicates that the transition from a bone-marrow-induced death to a GI syndrome-induced death occurs at a whole-body absorbed dose between 8.3 and 9.0 Gy.

Fig. 3*B* shows the survival of the beam-plus-liposome groups as a function of time after whole-body neutron beam irradiation with boronated liposomes in the blood. The estimated total absorbed doses in the vascular endothelial cells were 2- or 3-fold higher than the whole-body absorbed doses received by the crypt

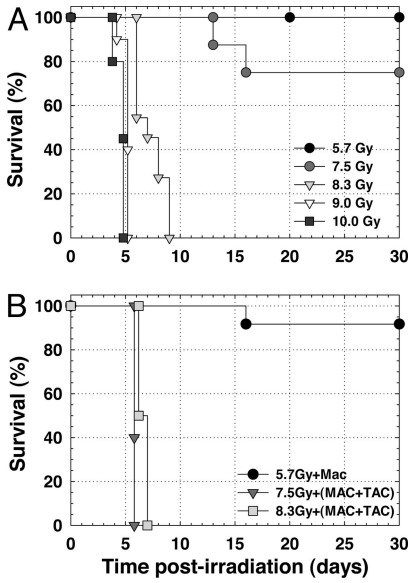

Fig. 3. Survival experiments. (*A*) Mouse survival after whole-body, neutron-beam-only irradiations. (*B*) Mouse survival after whole-body neutron irradiation with boronated liposomes present in the blood. The microvascular absorbed doses were 10.8 ± 0.9 (MAC), 25.0 ± 2.0 (MAC+TAC), and 27.7 ± 2.2 Gy (MAC+TAC), respectively.

stem cells (Table 1). In the 5.7-Gy beam plus MAC group, 11 of 12 mice lived beyond 30 d, whereas all mice (n = 10) in the 7.5-Gy beam plus MAC+TAC group and all mice (n = 8) in the 8.3-Gy beam plus MAC+TAC group died within 6–7 d. Fig. 4 shows hematoxylin-and-eosin-stained small intestine (jejunum) and bone marrow sections from a mouse in the 8.3-Gy beam plus MAC+TAC group killed 7 d after irradiation. The intestinal mucosa recovered, whereas the bone marrow was severely depleted, indicating that this mouse died from the bone marrow syndrome despite a physical absorbed dose in the microvasculature that exceeded 27 Gy.

The 7.5-Gy beam-only and 7.5-Gy beam plus MAC+TAC groups show considerably different survival times (Fig. 3), yet the mode of death was the same in both groups, namely, bone marrow depletion. The very high (>50 Gy) absorbed dose in the blood (see Table 1) in the presence of the MAC+TAC liposomes

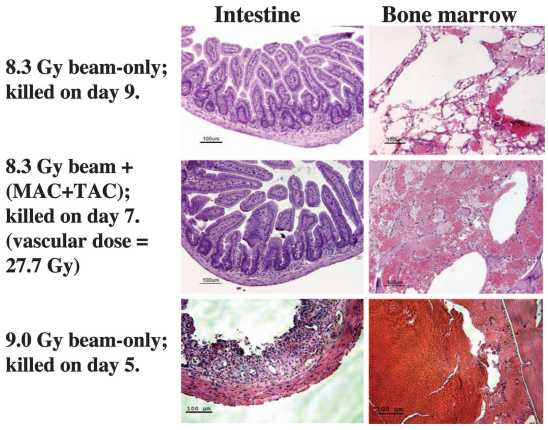

Fig. 4. Histopathology in small intestine and bone marrow after whole-body, neutron-beam-only absorbed doses of 8.3 ± 0.6 or 9.0 ± 0.6 Gy. Also shown are tissues from a mouse in the 8.3-Gy beam plus (MAC+TAC) liposomes group in which the calculated absorbed dose to the endothelial cells was 27.7 ± 2.2 Gy.

contributed enough dose to the bone marrow to cause a rapid death from the bone marrow syndrome. The exact mechanism of liposome-mediated delivery of boron into the bone marrow is not known.

Discussion

The cellular and subcellular events that eventually lead to the breakdown of tissue structure and function are initiated at the time of irradiation. Our ability to preferentially increase the absorbed dose to the vascular endothelial cells allows direct testing of the role played by microvascular damage in the subsequent development of normal tissue damage. We have established that whole-body neutron beam-only doses of ≈9.0 Gy represent the threshold for death from the GI syndrome. Our approach was to use neutron beam doses below the 9.0 Gy threshold for the GI syndrome in combination with boronated liposomes in the blood. The additional short-ranged boron neutron capture dose in the blood selectively increased the total absorbed dose in the microvasculature to values as high as 27.7 Gy, whereas the dose to the crypts remained <9.0 Gy. Despite these extremely high doses to the microvasculature, the crypt microcolony assay and histopathological confirmation of the mode of death indicated that all observed radiation effects in the small intestine could be attributed to the whole-body neutron beam dose: the added dose to the microvasculature was inconsequential. We conclude that damage to the intestinal microvasculature is not causative in the loss of stem cell function and the eventual depopulation of the intestinal lining that characterizes the GI syndrome.

The role of microvascular versus parenchymal cell damage has long been a matter of considerable debate for late effects (15–17). In recent years, it has become clear that the overall tissue response to radiation damage includes a complex interaction between the different cell types present that begins immediately after the radiation insult and persists throughout the clinically silent period until the expression of the late effect months or even years later. Radiation has been shown to result in the activation of a number of early response cytokines that act through diverse signaling pathways (18). This continuous cascade of cytokines has been proposed to induce a chronic inflammatory phase, which is in turn followed by late stromal alterations, such as fibrosis (19). Radiation injury has also been likened to a "complex wound" in which persistent damage to the vascular endothelium results in eventual dysregulation of the coagulation system, which in turn causes a chronic inflammatory response leading to fibrotic changes (20). Because of the lack of experimental techniques for selectively irradiating potential target populations to test these hypotheses, questions still remain as to which cell population(s) are the critical targets that initiate these signaling pathways, despite the increased understanding of the molecular responses in tissue to radiation exposure.

The present study is similar in concept to our previous work that addressed the role of vascular damage in the development of subacute and late effects in the CNS (9, 10). In those studies, the blood–brain (or spinal cord) barrier was used to keep a low-molecular-weight boron compound [$Na_2B_{12}H_{11}SH$ (BSH)] within the lumen of the blood vessels during neutron irradiation. In the spinal cord study (10), an *in vivo/in vitro* assay for O-2A glial progenitor cells showed that after uniform irradiation with the neutron beam alone the glial progenitor population was severely depleted at 1 week and remained so until the development of white matter necrosis and limb paralysis at 6 months after irradiation. In contrast, the glial progenitor population remained at high levels at all times after the irradiation with the neutron beam plus BSH in the blood. Both irradiation conditions were isoeffective for white matter necrosis (21). The conclusion from that study was that damage to the vascular endothelium was the primary event leading to white matter necrosis (10). In the rat brain study (9), at 30 d after irradiation, the loss of neural precursor cells and their progeny was shown to correlate with the absorbed dose in the brain parenchyma (the beam dose) and was not affected by the selective irradiation of the microvasculature (9). The results in the rat brain parallel what we report here for the acute loss of mouse intestinal crypt stem cells: The effect is direct and not mediated by the vascular dose.

The mixed high- and low-LET nature of the physical absorbed doses in the microvasculature reported here complicates a direct comparison to the low-LET doses used by Paris *et al*. (5). However, a biological weighting factor has been measured for BSH in the rat spinal cord using the myeloparesis endpoint (21), where white matter necrosis has been shown to be directly related to vascular damage (11, 12). BSH in the CNS produces the same ^{10}B distribution pattern as the liposomes in the intestine in the current study: The ^{10}B is restricted to the vessel lumen. The weighting factor derived in the rat spinal cord for BSH is 0.46 and converts the ^{10}B physical dose absorbed in the blood into a photon-equivalent dose to the vasculature (21). Application of the BSH weighting factor to the liposome ^{10}B blood doses (Table 1) generates estimated photon equivalent doses to the intestinal vasculature of 7.0, 24.2, and 26.8 Gy. In addition, the vasculature also received the nonspecific beam dose. Clearly, the upper range of the doses delivered to the vasculature in the beam-plus-liposome irradiations reported here are significantly higher than the 8- to 15-Gy photon dose used in the Paris *et al.* (5) study.

The proof-of-principle results described here suggest that our technique for selective vascular irradiation could be useful in other non-CNS tissues, such as the lung, where the role of vascular endothelial cell apoptosis as the initiating event in the development of lethal radiation pneumonitis in the mouse is a matter of debate (22, 23). This approach could also play an important role in studies of the molecular mechanisms leading to late fibrosis in tissues, such as the lung, the GI tract, or the kidney. Understanding the mechanisms that regulate early and late normal tissue radiation responses may have important implications and applications in the development of radiation protectors or treatments for radiation exposures.

Materials and Methods

Boron Analysis. The boron concentration in liquid or solid samples was determined by using the prompt gamma neutron activation analysis facility at the MIT reactor (24). This spectroscopic technique measures the prompt gamma ray emitted by the recoiling ^{7}Li nucleus after neutron capture in ^{10}B using a high-purity germanium detector. The system was calibrated by using boric acid certified by the National Institute of Standards and Technology and has a detection limit of ≈1 μg for ^{10}B. All stated uncertainties on ^{10}B measurements represent one standard deviation.

Liposomes. Two different ^{10}B-containing liposome formulations were used for these studies. Liposomes containing MAC embedded in the lipid bilayer were prepared as described in ref. 25. The water-soluble TAC polyhedral borane anion derivative can be incorporated into the interior of the liposome (26). MAC+TAC liposomes were prepared as described in ref. 27. All boron compounds were enriched in the ^{10}B isotope to >98%. The liposome formulations had a mean vesicle diameter between 70 and 90 nm and contained 24 mg of total lipid per milliliter. The MAC and the MAC+TAC liposome injection solutions were sterilized by passage through a 0.22-μm filter before use and contained 540 ± 27 μg/ml and 1,580 ± 79 μg/ml ^{10}B, respectively.

Animals and Animal Procedures. Female BALB/c mice, 8–12 weeks of age, were maintained in a 12-hour light/dark cycle and given food and water ad libitum. All procedures were reviewed and approved by the Committee on Animal Care at the Massachu-

setts Institute of Technology and were conducted according to the principles outlined in the Guide for the Care and Use of Laboratory Animals prepared by the Institute of Laboratory Animal Resources of the National Research Council.

Biodistribution Studies. The ^{10}B dose distribution is directly related to the ^{10}B concentrations in tissues at the time of irradiation. Liposome biodistribution studies were carried out to determine the amount of ^{10}B in blood, liver, skin, and small intestine as a function of time after injection. Twenty BALB/c mice were injected with 0.2 ml of the MAC liposome solution (108 μg of ^{10}B) via the retroorbital sinus while under brief isofluorane anesthesia. Five mice were killed by inhalation overdose of either isofluorane or carbon dioxide at each of four time points (15, 30, 45, and 60 min) after injection. Blood was drawn directly from the heart. The boron concentrations in blood and samples of skin (pinna), liver, and small intestine were measured by using prompt gamma neutron activation analysis. Eight mice received 0.2 ml of the MAC+TAC liposome solution (316 μg of ^{10}B) and were killed at 30 min after injection for boron analysis.

The boronated amino acid BPA was used to provide a uniform boron distribution in blood and tissues for a positive control experiment. Previous studies have shown that BPA distributes relatively uniformly from blood into normal tissues at 2–3 h after injection (28). The BPA was solubilized for injection as the fructose complex at a concentration of $\approx$83 mg/ml BPA (29). Five mice received a single injection of BPA (0.2 ml; 812 μg of ^{10}B) into the retroorbital sinus and were killed 2 h after injection for boron analysis.

Neutron Beam Irradiation. Whole-body mouse irradiations were carried out in the epithermal neutron beam at the Massachusetts Institute of Technology Nuclear Reactor Laboratory as described in ref. 14. Mice were irradiated in a Lucite holder designed to immobilize unanesthetized mice by the four feet such that the abdomens were presented to the 16-cm-diameter horizontal epithermal beam (14). Unless specifically noted, all doses quoted in this paper are physical absorbed doses to which no weighting factors have been applied. Absorbed doses ranging from 3.2 $\pm$ 0.2 to 10.0 $\pm$ 0.7 Gy were administered with irradiations lasting from 6 to 20 min. The epithermal neutrons were thermalized by 1.5 cm of Lucite, consisting of the 0.5-cm-thick mouse holder and an additional 1.0-cm sheet of Lucite placed between the holder and the beam aperture. The mouse bodies were centered at a depth of 2.5 cm. Photon and fast neutron absorbed dose rates were measured using paired ionization chambers with walls of graphite and tissue-equivalent A-150 plastic. The absorbed dose from neutron capture in ^{10}B and nitrogen was determined by using the measured difference in the activation of bare and Cd-covered gold foils and kerma coefficients of 8.66×10^{-8} and 7.88×10^{-12} Gy/cm^2, respectively. A uniform nitrogen concentration of 3.5% by weight was applied for tissue and boron concentrations measured in the biodistribution studies were used to determine the absorbed doses in the blood and vessel wall (30).

Vascular Dose Calculations. The boron neutron capture reactions in the liposome groups occur, by design, only within the vessel lumen. This creates a nonuniform dose distribution in which the dose delivered to the vascular endothelium is less than the boron dose absorbed in the blood volume within the lumen. Rydin *et al.* quantified this effect of vessel geometry on the dose absorbed in an endothelial cell from boron neutron capture reactions restricted to the lumen of a blood-filled capillary relative to the boron dose absorbed in the blood (13). According to this model, when ^{10}B is restricted to the lumen, the boron dose absorbed in the capillary wall is one-third of the boron dose absorbed in the blood given a capillary wall thickness of 0.25 μm, which is considered representative for the mice used in this study. The total physical absorbed dose in the vascular endothelium is the sum of the external beam dose and the vascular-specific boron dose.

Crypt Regeneration Assay. The intestinal crypt microcolony assay (3) was used to quantify the effects of the different absorbed dose distributions delivered to the microvasculature and to the intestinal crypt stem cells. This assay has several advantages, such as a steep dose–response relationship and independence from the dose to adjacent normal tissues. Based on its sensitivity, it has been used to quantify the different biological effects of clinical fast neutron therapy beams differing in radiation quality by no more than $\approx$10% (31). In the studies reported here, mice received whole-body, neutron-beam irradiation either without administered boron, 30 $\pm$ 5 min after a 0.2-ml liposome injection, or 2 h after injection of BPA. The mice were killed 84 $\pm$ 1 h after irradiation, and a 5-cm section of the jejunum was removed, cut into 0.5-cm segments, and placed into 10% formalin fixative for 24–48 h. After fixation, the intestine sections were embedded vertically in paraffin to generate cross sections when cut and then stained with hematoxylin and eosin. The numbers of regenerating crypts per circumference were counted, with at least four sections per mouse and four mice per dose point. The criteria used for scoring a regenerating crypt were 10 or more contiguous epithelial cells and at least one Paneth cell (2, 3). No correction factor was applied, because the average crypt size in all irradiated groups was the same. A single, blinded observer scored all slides.

Survival Studies. Mouse survival experiments were carried out at the following absorbed doses of a whole-body epithermal neutron beam: 5.7 $\pm$ 0.4, 7.5 $\pm$ 0.5, 8.3 $\pm$ 0.6, 9.0 $\pm$ 0.6, and 10.0 $\pm$ 0.7 Gy. At the three lowest doses, groups of 8–12 mice received either beam-only irradiation or irradiation together with boronated liposomes in the blood. The MAC liposomes were used for the 5.7-Gy dose level, and the MAC+TAC liposomes were used for the 7.5- and 8.3-Gy dose levels. No boronated liposomes were administered for the 9.0- and 10.0-Gy dose levels. Mice were weighed daily after irradiation and killed upon entering a moribund state. Intestine and femur samples were harvested for histology to ascertain the likely mode of death.

This work was supported in part by the U.S. Department of Energy Nuclear Engineering and Health Physics Fellowship Program (B.W.S.) and by Innovations in Nuclear Infrastructure and Education Program Contract DE-FG07-02ID14420, both of which are sponsored by the U.S. Department of Energy's Office of Nuclear Energy, Science, and Technology. Additional support was provided by National Institutes of Health Grant 1R01 CA97342-01A2 (to M.F.H.), the Westaway Family Memorial Fund at Massachusetts Institute of Technology (J.A.C.), and the Massachussetts Institute of Technology Center for Environmental Health Sciences through National Institute of Environmental Health Sciences Grant ES002109.

1. Potten, C. S., Booth, C., Tudor, G. L., Booth, D., Brady, G., Hurley, P., Ashton, G., Clarke, R., Sakakibara, S. & Okano, H. (2003) *Differentiation (Berlin)* **71,** 28–41.
2. Potten, C. S. (2004) *Radiat. Res.* **161,** 123–136.
3. Withers, H. R. & Elkind, M. M. (1970) *Int. J. Radiat. Biol. Relat. Stud. Phys. Chem. Med.* **17,** 261–267.
4. Hornsey, S. (1973) *Radiat. Res.* **55,** 58–68.
5. Paris, F., Fuks, Z., Kang, A., Capodieci, P., Juan, G., Ehleiter, D., Haimovitz-Friedman, A., Cordon-Cardo, C. & Kolesnick, R. (2001) *Science* **293,** 293–297.
6. Ch'ang, H. J., Maj, J. G., Paris, F., Xing, H. R., Zhang, J., Truman, J. P., Cardon-Cardo, C., Haimovitz-Friedman, A., Kolesnick, R. & Fuks, Z. (2005) *Nat. Med.* **11,** 484–490.
7. Maj, J. G., Paris, F., Haimovitz-Friedman, A., Venkatraman, E., Kolesnick, R. & Fuks, Z. (2003) *Cancer Res.* **63,** 4338–4341.

8. Kolesnick, R. & Fuks, Z. (2003) *Oncogene* **22,** 5897–5906.
9. Otsuka, S., Coderre, J. A., Micca, P. L., Morris, G. M., Hopewell, J. W., Rola, R. & Fike, J. R. (2006) *Radiat. Res.* **165,** in press.
10. van der Kogel, A. J., Kleiboer, B. J., Verhagen, I., Morris, G. M., Hopewell, J. W. & Coderre, J. A. (1996) in *Radiation Research 1895–1995*, eds. Hagen, U., Harder, D., Jung, H. & Streffer, C. (Sturtz, Wurzburg, Germany), Vol. 2, pp. 769–772.
11. Morris, G. M., Coderre, J. A., Bywaters, A., Whitehouse, E. & Hopewell, J. W. (1996) *Radiat. Res.* **146,** 313–320.
12. Morris, G. M., Coderre, J. A., Whitehouse, E. M., Micca, P. & Hopewell, J. W. (1994) *Int. J. Radiat. Oncol. Biol. Phys.* **28,** 1107–1112.
13. Rydin, R. A., Deutsch, O. L. & Murray, B. W. (1976) *Phys. Med. Biol.* **21,** 134–138.
14. Gueulette, J., Binns, P. J., Coster, B. M., Lu, X. Q., Roberts, S. A. & Riley, K. J. (2005) *Radiat. Res.* **164,** 805–809.
15. Withers, H. R., Peters, L. J. & Kogelnik, H. D. (1980) in *Radiation Biology in Cancer Res.*, eds. Meyn, R. E. & Withers, H. R. (Raven, New York), pp. 439–448.
16. Calvo, W., Hopewell, J. W., Reinhold, H. S. & Yeung, T. K. (1988) *Br. J. Radiol.* **61,** 1043–1052.
17. Hopewell, J. & Withers, H. R. (1998) *Med. Phys.* **25,** 2265–2268.
18. Rubin, P., Johnston, C. J., Williams, J. P., McDonald, S. & Finkelstein, J. N. (1995) *Int. J. Radiat. Oncol. Biol. Phys.* **33,** 99–109.
19. Okunieff, P., Cornelison, T., Mester, M., Liu, W., Ding, I., Chen, Y., Zhang, H., Williams, J. P. & Finkelstein, J. (2005) *Int. J. Radiat. Oncol. Biol. Phys.* **62,** 273–278.
20. Denham, J. W. & Hauer-Jensen, M. (2002) *Radiother. Oncol.* **63,** 129–145.
21. Morris, G. M., Coderre, J. A., Hopewell, J. W., Micca, P. L., Nawrocky, M. M., Liu, H. B. & Bywaters, A. (1994) *Radiother. Oncol.* **32,** 249–255.
22. Fuks, Z., Persaud, R. S., Alfieri, A., McLoughlin, M., Ehleiter, D., Schwartz, J. L., Seddon, A. P., Cordon-Cardo, C. & Haimovitz-Friedman, A. (1994) *Cancer Res.* **54,** 2582–2590.
23. Tee, P. G. & Travis, E. L. (1995) *Cancer Res.* **55,** 298–302.
24. Riley, K. & Harling, O. (1998) *Nucl. Instrum. Meth. Phys. Res., Sect. B* **143,** 414–421.
25. Feakes, D. A., Shelly, K. & Hawthorne, M. F. (1995) *Proc. Nat. Acad. Sci. USA* **92,** 1367–1370.
26. Feakes, D., Shelly, K., Knobler, C. & Hawthorne, M. (1994) *Proc. Natl. Acad. Sci. USA* **91,** 3029–3033.
27. Watson-Clark, R. A., Banquerigo, M. L., Shelly, K., Hawthorne, M. F. & Brahn, E. (1998) *Proc. Natl. Acad. Sci. USA* **95,** 2531–2534.
28. Coderre, J. A. & Morris, G. M. (1999) *Radiat. Res.* **151,** 1–18.
29. Coderre, J. A., Button, T. M., Micca, P. L., Fisher, C. D., Nawrocky, M. M. & Liu, H. B. (1994) *Int. J. Radiat. Oncol. Biol. Phys.* **30,** 643–652.
30. Riley, K. J., Binns, P. J. & Harling, O. K. (2003) *Phys. Med. Biol.* **48,** 943–958.
31. Gueulette, J., Octave-Prignot, M., De Costera, B. M., Wambersie, A. & Gregoire, V. (2004) *Radiother Oncol.* **73,** Suppl. 2, S148–S154.